

In situ gold-nanoparticle electrogeneration on gold films deposited on paper for non-enzymatic electrochemical determination of glucose

Estefanía Núñez-Bajo

M. Carmen Blanco-López

Agustín Costa-García

M. Teresa Fernández-Abedul*

mtfernandez@uniovi.es

Departamento de Química Física y Analítica, Facultad de Química, Universidad de Oviedo, 33006 Oviedo, Spain

*Corresponding author.

Abstract

This work describes the development and evaluation of a new electrochemical platform based on the sustainable generation of gold-nanoparticles on paper-based gold-sputtered electrodes. The disposable porous paper electrode is combined with screen-printed electrodes for ensuring a precise electrogeneration of nanoparticles and also for the evaluation of these simple, versatile and low-cost microfluidic devices. Two types of chromatographic paper with different thicknesses have been evaluated. Resulting paper gold working electrodes modified with gold nanoparticles were characterized by scanning electron microscopy and cyclic voltammetry using potassium ferrocyanide as a common redox probe, showing an improved electrochemical performance when compared to the bare gold electrodes. The platform has been applied to the non-enzymatic determination of glucose, molecule of enormous interest. The porous gold structure made by paper sputtering on paper, modified with electrogenerated nanoparticles allowed precise and accurate determination of the analyte in beverages at low potential.

Keywords: electroanalytical Electroanalytical paper-based devices; nanostructured Nanostructured paper-based devices; gold-sputtered Gold-sputtered electrodes; electrogenerated Electrogenerated gold nanoparticles; low-cost Low-cost decentralized analysis; non-enzymatic Non-enzymatic glucose analysis

1 Introduction

This is the golden age of electrochemistry, a field at the nexus of many developing technologies [1]. In this area, energy storage devices and electroanalytical platforms are being widely explored. This is mainly due to the advances in materials and their uses [2,3] and also into the design of miniaturized platforms [4,5] that open the field to new opportunities. Particularly, electroanalysis has moved from the use of conventional cells that include mercury and solid (metallic or carbon) electrodes to other with more advantageous electrodes. Glass or polymeric cylinders that were commonly the body support of the conductive elements (e.g., carbon paste [6] and incorporated with an inner connection to the potentiostat turned into flat surfaces where all the three electrodes are included in a small area [7,8]. A container is not required since e.g., a dielectric layer [9] or just the hydrophobicity of the substrate [10] eliminates its necessity.

However, although their small size and mass-production widespread the use of these ceramic or polymer-based devices, it was not until Whitesides' group introduced microfluidic paper-based analytical devices (μ PADs) [11] where a new milestone was set. The first electrochemical paper-based analytical device (ePAD) [12] was rapidly followed by different electrochemical transducers [10,13-26]-18. Apart from the coupling of wires or fibers [15,20,21], thin and thick-film technologies are employed to integrate conductive materials into paper substrates. Noble metal electrodes are an alternative to carbon [10,14,16,22,23] electrodes and can be easily obtained using thin-film technologies [17,24-26] that maintain the 3D porous structure of paper and do not require printing inks or curing processes.

On the other hand, different nanostructures, mainly carbon nanotubes [27], graphene [28] or metallic nanoparticles [29] have been used as electrodes themselves or as modifiers of electrodes in ePADs. The electrodeposition of nanoparticles offers the possibility of in situ generation on the working electrode in a simple, fast, more reproducible, controlled and localized way, in the working electrode. In addition, electrochemical generation of gold nanoparticles (AuNPs) does not require ligands such as citrates to stabilize the resulting nanoparticles [30]. In this ligand-free approach, the surface of the nanoparticles is not covered by molecules that decrease their specific surface activity. However, most researchers use wet chemistry in ePADs [31-33], and although AuNPs-modified paper-based carbon electrodes have been reported, e.g., for As determination [23], there are no references on any gold thin-film

ePAD modified with gold nanoparticles (neither by wet chemistry or electrodeposition).

Gold is a material with characteristics differing from those of carbon and they can be exploited for interesting applications: i) simple immobilization chemistries, e.g., self-assembly of thiol-labelled molecules [34] being this metal reasonably inert [35], ii) differential electrochemical behavior, e.g., the reduction of chromium (VI) produces an electrochemically reversible wave in gold, in contrast to those recorded at glassy carbon [36]; or iii) adsorption of species, e.g., heteropolyanions, that occurs with different intensity depending on the electrode material [37].

As a proof-of-concept, we tested the feasibility of ~~the~~ gold ePAD modified with (AuNPs) to determine glucose. Non-enzymatic determination of small molecules is an area of continuous interest [38,39] and electrode nanostructuring is one of the explored ways [40]. Apart from other nanoparticles, AuNPs were evaluated with this aim, not only on carbon but also on gold electrodes [41]. Interestingly, glucose can be partially oxidized at bulk Au electrodes [42] and several carbon nanogold electrodes for non-enzymatic glucose sensors have been developed [43,44]. In our case, the paper acts as a porous template for sputtered gold, that facilitates mass transport. On the other hand, AuNPs increase the active area favoring rapid electrochemical reactions. This 3D porous nanostructured material is employed for the first time for non-enzymatic glucose determination using disposable low-cost platforms that are a promising alternative to AuNPs-carbon ePADs for decentralized analysis.

2 Experimental

2.1 Chemicals, materials and apparatus

Potassium ferrocyanide trihydrate ($K_4[Fe(CN)_6] \cdot 3H_2O$) was purchased from Sigma-Aldrich. Sodium hydroxide, potassium chloride, ~~and~~ orthophosphoric acid (90%) ~~and~~ anhydrous D-(+)-glucose, ~~were supplied by Merck~~ and Titrisol® Gold-Standard (10.15 mM $AuCl_4^-$ in 2.0 M HCl solution) ~~and potassium chloride~~ were supplied by Merck. All the solutions were prepared in Milli-Q water (Merck Millipore).

Whatman chromatographic papers grade 1 (180- μ m thick) and grade 3MM (260- μ m thick) were obtained from GE Healthcare Life Sciences. Screen-printed carbon electrodes (SPCEs) model DS110 were manufactured by DropSens.

A Sputtering DC model CD 004 from Balzers was employed for gold deposition. Electrochemical measurements were made using an Autolab PGSTAT potentiostat model (PGSTAT12) from Metrohm (USA). A Mettler Toledo (AB54) balance, a Crison Micro-pH 2001 pH-meter, a magnetic stirrer Asincro (J.P. Selecta), Digital Multimeter Model (DT9205A) were also employed.

2.2 Fabrication of paper-based gold electrodes

All the steps are schematized in Fig. 1. Whatman chromatographic paper was wax-printed with a pattern designed with Adobe Illustrator CC software. The pattern consisted of 6-mm diameter circles with 0.7 mm of drawing stroke in order to obtain circles of 4 mm radius after wax melting in a hot plate at 110 °C during 2 min to create hydrophobic barriers. Once the wax was melted, the sheets were cut into 60 mm \times 75 mm pieces. A plastic sheet was placed under the paper as a backing protective layer. This ensemble was covered with gold in a sputtering process, with a 20-mA discharge applied for 240 s. Then, the backing was removed and ~~the~~ conductive layers were protected with plastic covers (4-mm diameter circles of transparency film). Adhesive spray was deposited on the hydrophobic wax area. Covers were removed and sheets were cut into conductive ~~and~~ adhesive discs (4 mm-diameter hydrophilic area and 0.5-mm hydrophobic adhesive rim) using a paper punch.

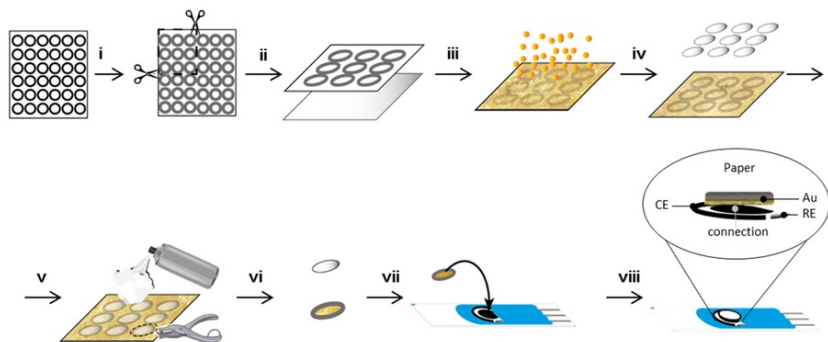


Fig. 1 Schematic representation of the fabrication and coupling of paper-based gold working electrodes (PAuWEs): (i) wax-melting after wax-printing, (ii) cutting and protection with a plastic sheet, (iii) gold sputtering, (iv) protection of the conductive layer with plastic covers, (v) addition of adhesive in spray, (vi) removal of plastic cover after cutting the PAuWE, (vii) placement over the working electrode of the SPCE, (viii) final platform composed by the PAuWE with external reference and counter electrodes from the SPCE.

Gold paper electrodes were then combined with SPEs, fixing the paper on the working electrode (WE), which acted as connection to the potentiostat. This was previously washed with Milli-Q water and dried. The adhesive side was placed over the ceramic card in such a way that the conductive layer is in direct contact with the carbon spot and the adhesive part is just on the ceramic circular crown situated between working and counter/reference electrodes. Taking into consideration ~~that~~ the adhesive is not hydrophilic and ~~that it~~ is placed in between ~~the~~ electrodes, contamination is not ~~probable~~~~expected~~. The upper side is porous paper where the solution is dropped. ~~It and~~ arrives to the inner gold part of the paper by capillarity. The silver pseudo-reference and carbon counter electrodes of the SPCE card acted as external electrodes. In order to compare the electrochemical behavior of glucose using AuNPs paper-based carbon electrodes, drop-casted carbon electrodes were prepared as reported in a previous work [23].

2.3 Characterization of paper-based gold electrodes modified with gold nanoparticles

Cyclic voltammetry (CV) was performed in $K_4Fe(CN)_6$ solutions in 0.1 M phosphate buffer (PB) pH 7.0 with 0.1 M KCl scanning the potential from -0.1 to $+0.5$ V vs. the pseudo-reference electrode of the SPE at a scan rate of 100 mV s⁻¹.

In addition, the topography of the PWEs and AuNPs-PWEs was examined by scanning electron microscopy (SEM). For these studies, samples were placed perpendicularly to the electron beam with a working distance of 10 mm and 20 kV of extraction tension in a JEOL (model 6610LV) microscope.

2.4 Glucose determination in real samples

In order to know the electrochemical behavior of D-(+)-glucose using the modified paper-based gold electrodes, CVs (and linear sweep voltammograms, LSVs) were recorded on 50- μ L D-(+)-glucose solutions in 0.1 M NaOH scanning the potential in different windows at a scan rate of 100 mV s⁻¹.

Real samples were diluted conveniently in 0.1 M NaOH and 50- μ L aliquots were deposited on the integrated platforms (AuNPs-PAuWE-SPCE), with all the electrodes covered. CVs were recorded scanning the potential from -0.3 to $+0.5$ V at a scan rate of 100 mV s⁻¹. Determination of the concentration was made by comparison with an external calibration curve. In order to test the accuracy of the results obtained, samples were also analyzed using a commercial glucose kit with spectrophotometric detection.

3 Results and Discussion

3.1 Fabrication and characterization of nanostructured paper-based gold electrodes

A paper-based gold-sputtered ~~paper~~~~working~~ electrode (PAuWE) was employed as the substrate for sustainable generation of gold nanoparticles (AuNPs) constituting a new porous electrochemical platform. For the nanostructuring, no extra reducing agents are required since nanoparticles are generated by electrochemical reduction of $AuCl_4^-$. This ensures an intimate electrical connection to the gold film. Whatman chromatographic papers ~~G~~ grade 1 and 3 MM were evaluated. Although a paper-fully-based three electrode cell could be employed, SPCEs are robust platforms that can be employed as support for nanostructuring paper and, alternatively, also to perform analyte determination. Although SPEs can break, one advantage is that they do not need any ~~physical~~~~physical~~ support, they are mechanically more stable than paper (in the case of paper this could be achieved by previous silanization [10]) and they can be easily washed and dried. Individual modification of the working electrode can be made and, if no adsorption occurs on the carbon surface, ~~it~~~~they~~ could be reused. Moreover, they incorporate a silver electrode, that although pseudo-reference, produces stable potentials for the generation of nanoparticles.

For the electrogeneration, direct reduction of Au(III) to Au(0) on the electrode surface is performed, galvanostatic or potentiostatically. Better results, ~~in terms of precision~~, were obtained with the first procedure, previously employed in our group ~~with on~~ SPEs [45], ~~in terms of precision~~. A constant current of -100 μ A that produces the reduction of Au(III) to Au(0) is applied during different times in a 10.15 mM acidic solution of $AuCl_4^-$ (2.0 M in HCl).

Before using AuNPs-PAuWEs for electroanalytical purposes, they are washed with Milli-Q water to reduce the capacitive current (Fig. 2A, inset). The charge of the electric double layer, responsible for the magnitude of this current, depends on several parameters such as: electrode material, supporting electrolyte, specific adsorption of ions and molecules, and temperature, with its thickness depending on the bulk electrolyte concentration and the ion charge among other factors [46]. Since all the variables remain very similar, the adsorption of ions and molecules (including $AuCl_4^-$ ions, present mainly before washing, in equilibrium with Au^{3+} and Cl⁻) seem to be the main responsible for the change in the capacitive current ~~before and~~ after washing.

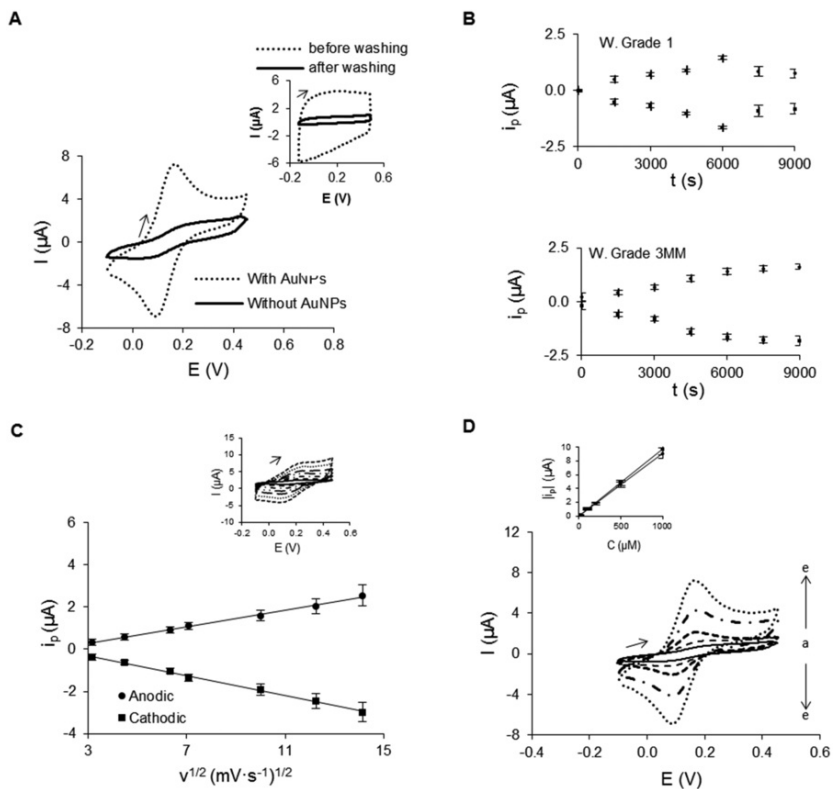


Fig. 2 (A) CVs recorded in 0.1 M PB (pH 7.0) with 0.1 M KCl before and after the washing step (inset) and in 1 mM $K_4Fe(CN)_6$ solution in 0.1 M PB (pH 7.0) with 0.1 M KCl using an unmodified PAuWE and a AuNPs-PAuWE coupled to SPCEs. (B) Anodic and cathodic peak currents obtained by CV in $100 \mu M$ $K_4[Fe(CN)_6]$ solutions using AuNPs-PCWEs in Whatman Grade 1 and 3 MM papers where AuNPs were generated galvanostatically with different times. Potential swept from -0.1 to $+0.5$ V vs. Ag pseudo-reference at 100 $mV s^{-1}$. (C) Effect of the scan rate on peak currents obtained recording CVs (inset) in a $100 \mu M$ $K_4Fe(CN)_6$ solution in 0.1 M PB (pH 7.0) with 0.1 M KCl at several scan rates: 10, 25, 40, 50, 100, 150 and 200 $mV s^{-1}$ using AuNPs-PAuWEs coupled to SPCEs. (D) CVs recorded sweeping the potential from -0.1 V to $+0.5$ V at a scan rate of 100 $mV s^{-1}$ in $K_4Fe(CN)_6$ solutions of different concentration, increasing from a to e. Inset: Calibration plots of anodic and cathodic peak currents.

alt-text: Fig. 2

The electrochemical behavior of resulting platforms was tested by CV using a 1 mM solution of $K_4Fe(CN)_6$ in 0.1 M phosphate buffer (PB) pH 7.0, 0.1 M in KCl, as a well-known redox probe. A 50- μL solution was deposited on the paper and three CVs were recorded at 100 $mV s^{-1}$. The faradaic process of the ferro/ferri system using bare PAuWEs and the nanostructured AuNPs-PAuWEs is shown in Fig. 2A. The intensity of the current increases ten times for nanostructured AuNPs-PAuWEs in comparison to unmodified PAuWEs and also reversibility is enhanced. Moreover, the ratio between anodic and cathodic peak currents changed from 0.80 ± 0.05 (PAuWEs) to 0.99 ± 0.05 (AuNPs-PAuWEs). The values for the currents (anodic and cathodic respectively) obtained on AuNPs-PAuWEs were 4.72 ± 0.09 and -4.76 ± 0.12 μA respectively, meanwhile these values were of 0.67 ± 0.13 and -0.82 ± 0.11 μA on unmodified electrodes. The difference between anodic and cathodic potentials changed from this of a quasi-reversible process, 110 ± 6 mV, to this of an almost reversible process, 64 ± 4 mV. Therefore, these platforms seem to be very convenient for electroanalysis since the faradaic current is notably increased as well as the reversibility of the process. Optimization of electrodeposition variables was carried out nanostructuring PAuWEs in triplicate and recording CVs in 10.15 mM $AuCl_4^-$ acidic solution. Currents of -10 , -20 , -50 and -100 μA were checked for 1000 s, obtaining better results with the highest value of current. Similarly, -100 μA were applied and electrolysis was maintained for times comprised between 1500 and 9000 s in both Whatman papers, followed by three washings with Milli-Q water. Peak currents obtained in CVs recorded in $100 \mu M$ $K_4[Fe(CN)_6]$ solution are shown in Fig. 2B. A time of 6000 s was appropriate to generate gold nanostructures on Whatman Grade 1 PAuWEs because high and precise signals are obtained. Higher times produce a decrease in peak currents and precision, which may be indicative of gold detachment. On the other hand, thicker and more expensive Whatman Grade 3 MM required the same time for obtaining similar currents. In all the cases, there is a significant increase (ca. 48 and 7 times for Grade 1 and 3 MM, respectively) compared to the unmodified PAuWE (first point of the plots in Fig. 2B), which can be promising for increasing the sensitivity of electroanalytical platforms. Whatman Grade 1 PAuWEs were employed as substrates for electrogeneration

of AuNPs.

In order to know the nature of the redox process on this new platform, the dependence of the peak current on the scan rate was evaluated in 100 μM $\text{K}_4\text{Fe}(\text{CN})_6$ solutions. CVs were recorded for three different AuNPs-PAuWEs coupled to SPCEs (Fig. 2C, inset). A linear relationship was found when peak currents were represented vs. the square root of the scan rate between 10 and 200 mV s^{-1} (Fig. 2C) with $R^2 = 0.9953$ and 0.9964 for anodic and cathodic peak currents respectively. This indicated that the reversible process takes place under mass transfer regime of semi-infinite diffusion control. However, it can be seen that there is lower peak potential separation at lower scan rates (it moves from 31 to 700 mV when scan rate varies from 10 to 200 mV s^{-1}), which can be indicative of the introduction of kinetic control on the shorter time scale or a small amount of uncompensated resistance. The influence of the concentration on the peak currents was evaluated from 1 to 1000 μM (Fig. 2D). The linear calibration plots are shown in the inset, each point being the average of three different devices. Equations were $i_{\text{pa}} (\mu\text{A}) = 0.0091 C (\mu\text{M}) + 0.0045$ and $|i_{\text{pc}}| (\mu\text{A}) = 0.0097 C (\mu\text{M}) - 0.0073$. Good linearity ($R^2 > 0.9995$) was observed in all the range indicating this platform could be satisfactorily employed as in a new generation of electroanalytical sensors.

Once the gold nanostructuring on PAuWEs was optimized, the morphology of the AuNPs generated on Whatman grade 1 PAuWEs was studied by scanning electron microscopy. Fig. 3A-C compare the morphological features of the unmodified PAuWE with those of a AuNPs-PCWE obtained electrodepositing gold for 6000 s. Fig. 3A shows a SEM image of a PAuWE cross-section after depositing gold by the sputtering process, where a network of fibers is observed. After nanostructuring (Figs. 3B and 3C, different scale), AuNPs connected to the gold surface on the cellulosic fibers. The average diameter ($56 \pm 16 \text{ nm}$) was estimated taken from the amplified image (20 samples). Clusters of $170 \pm 44 \text{ nm}$ are also found in some regions.

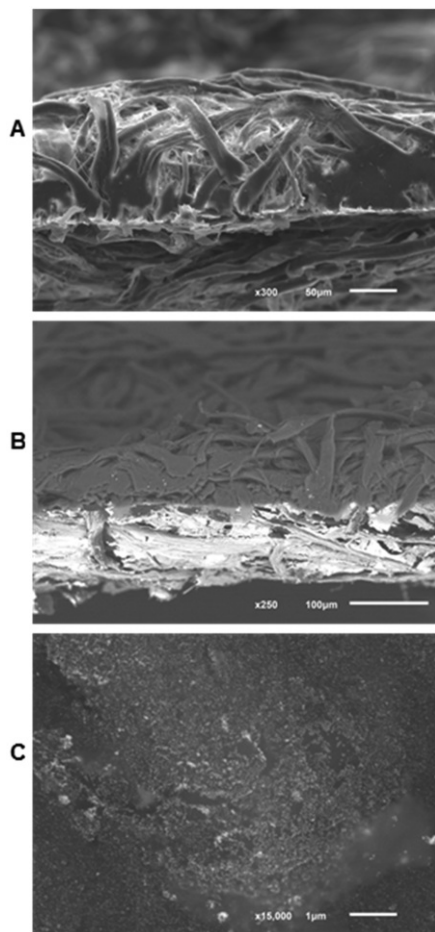


Fig. 3 Scanning electron microscopy cross-section images of a PAuWE $\times 300$ (A), AuNPs-PAuWEs $\times 250$ (B), and AuNPs-PAuWEs $\times 15000 \times 15000$ (C).

alt-text: Fig. 3

3.2 Non-enzymatic determination of glucose with nanostructured paper-based gold electrodes

Once paper-based electrodes have been nanostructured, their usefulness and applicability was demonstrated through the non-enzymatic determination of glucose by CV. Generally, the use of enzymes increases the cost of the devices and the precision could be compromised if the bioactivity is not guaranteed. Fig. 4A shows CVs recorded in 10 mM glucose solutions in 0.1 M NaOH on different paper electrodes: drop-casted carbon and sputtered gold. Comparison between bare and nanostructured electrodes (with AuNPs) is also shown. There is no signal for glucose oxidation on the bare carbon electrode. However, the bare gold electrode (PAuWE) showed two anodic peaks (at ca. +0.080 and +0.220 V). Then, this is an example that indicates that the use of gold electrodes is required for some specific applications. At lower concentrations of glucose only one peak appears. The presence of a second process could be due to an adsorption post-wave. A two-step mechanism has been suggested for glucose electrooxidation in alkaline solution on bulk gold electrode [42], with electrosorption of glucose by dehydrogenation in basic medium and further oxidation to gluconolactone that is later hydrolyzed to gluconic acid [42,43]. It can be observed that gold possesses lower overpotential for hydrogen evolution. The signal on the AuNPs-PAuWE is higher than that of the unmodified PAuWE. Although nanostructuring of drop-casted carbon paper electrodes (AuNPs-PCWEs) has been very convenient for different applications (e.g., arsenic determination [23]) and permit oxidation of glucose, it does not allow to obtain higher signals than those presented on AuNPs-PAuWEs.

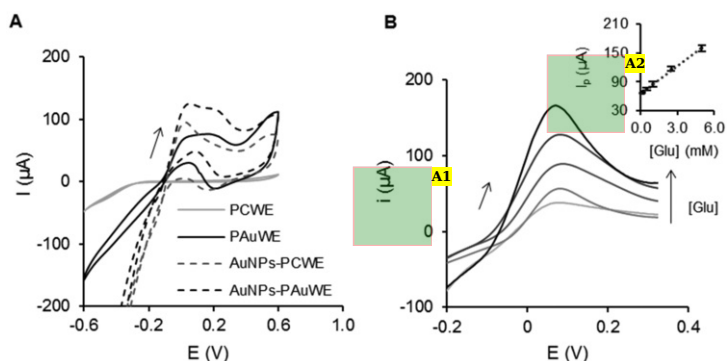


Fig. 4 (A) CVs recorded at 100 mV s^{-1} in 10 mM D-(+)-glucose solutions in 0.1 M NaOH on different paper-based electrodes coupled to SPCEs. (B) LSVs recorded for different concentrations of D-(+)-glucose (0.01, 0.1, 1.0, 2.5 and 5 mM) in 0.1 M NaOH using AuNPs-PAuWEs coupled to SPCEs. The calibration plot is shown in the inset. Data are given as average \pm SD ($n=3$), ($n=3$). Potential is scanned at 100 mV s^{-1} . (C) Results of the determination of glucose in real samples using three different methodologies. Data are given as average \pm SD ($n=3$) for AuNPs-PAuWEs and spectrophotometric methodologies and $n=4$, $n=4$ for PCWEs).

alt-text: Fig. 4

Annotations:

A1. I instead of i

A2. I instead of i

Glucose oxidation process obtained at the lowest potential (+0.080 V) is a better peak for precise determination without interferences from fructose and sucrose (data not shown) and therefore, it was here employed. A calibration curve performed in the range comprised between 0.01 and 5 mM, is presented in Fig. 4B, with each point the average of three measurements. A linear relationship was obtained with a $R^2 = 0.998$. The slope and intercept were $19.01 \pm 0.04 \text{ } \mu\text{A mM}^{-1}$ and $66.4 \pm 0.3 \text{ } \mu\text{A}$, respectively. The limit of detection (LOD) calculated according to the $3S_b / m$ criterium, where S_b is the standard deviation of the intercept and m is the slope of the linear range, was $6 \text{ } \mu\text{M}$.

Real samples of orange juice, cola and energetic beverages were analyzed using AuNPs-PAuWEs and the results were compared with those obtained using a commercial enzymatic kit with spectrophotometric detection and with those obtained enzymatically with an electroanalytical platform containing a PCWE and wire reference and counter electrodes [15]. Results obtained by the different methodologies are shown on Table 1. The application of the t -Student's test demonstrates that there were no significant differences between the values given by the commercial kit and our paper platforms at a 0.05 significance level. Good accuracy and precision of this methodology reveal a

promising future for these low-cost electroanalytical platforms.

Table 1 Results for the determination of glucose in real samples using the methodology here proposed (non-enzymatic, AuNPs-PAuWEs), a commercial enzymatic kit with spectrophotometric detection and an electrochemical platform based on AuNPs-PCWEs with wire RE and CE (enzymatic assay).

alt-text: Table 1

Real sample	AuNPs-PAuWEs on SPCEs (non-enzymatic, g/100 mL)	PCWEs with wire RE and CE (enzymatic, g/100 mL)	Commercial kit (g/100 mL)
Orange juice	2.8 ± 0.4	3.0 ± 0.3	2.9 ± 0.2
Energetic beverage	3.4 ± 0.3	3.6 ± 0.4	3.5 ± 0.2
Cola beverage	4.0 ± 0.5	4.2 ± 0.7	4.1 ± 0.3

Data are given as average \pm SD (n = 3 for AuNPs-PAuWEs and the spectrophotometric kit; n = 4 for PCWEs).

4 Conclusions

Paper-based gold working electrodes are combined with SPCEs for reproducible electrochemical generation of gold nanoparticles. Although a different platform could be employed [21], SPCEs are also useful for detection. Ferrocyanide, a well-known redox probe, was employed for evaluation of the final platforms. Since its redox process was notoriously improved when AuNPs are employed, the use of AuNPs-PAuWEs in bioassays involving the use of ferrocyanide as mediator is promising. On the other hand, we have demonstrated its potential for non-enzymatic glucose determination. Glucose is directly measured by LSV on AuNPs-PAuWE-SPCEs at low potentials. The limit of detection was 6 μ M with a linear range comprised between 0.01 and 5 mM. Glucose was determined in real food samples precise and accurately, which encourages us to extend its use to different applications.

Acknowledgements

This work has been supported by the Spanish Ministry of Economy and Competitiveness (MINECO) under projects CTO2011-25814 and CTO2014-58826-R. Estefania Núñez-Bajo thanks MINECO for the award of Ph.D. grant BES-2012-056713.

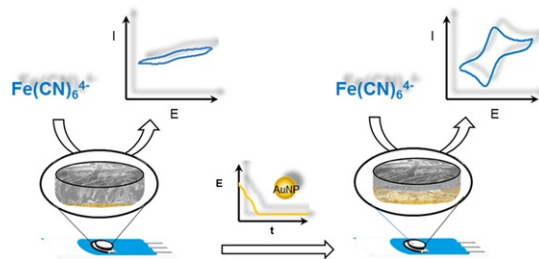
References

- [1] R.M. Penner and Y. Gogotsi, The rising and receding fortunes of electrochemists, *ACS Nano* **10**, 2016, 3875-3876.
- [2] D.C. Christodouleas, F.C. Simeone, A. Tayi, S. Targ, J.C. Weaver, K. Jayaram, M.T. Fernández-Abedul and G.M. Whitesides, Fabrication of paper-templated structures of noble metals, *Adv. Mater. Technol.* **2017**, 1600229, available online.
- [3] M.M. Hamed, A. Ainla, F. Güder, D.C. Christodouleas, M.T. Fernández-Abedul and G.M. Whitesides, Integrating electronics and microfluidics on paper, *Adv. Mater.* **28**, 2016, 5054-5063.
- [4] (www.micruxfluidic.com) (last access on August 2017).
- [5] E. Costa-Rama, A. Costa-García and M.T. Fernández-Abedul, Pin-based flow injection electroanalysis, *Anal. Chem.* **88**, 2016, 9958-9963.
- [6] M.T. Fernández-Abedul, J.R. Barreira-Rodríguez, A. Costa-García and P. Tuñón-Blanco, Voltammetric determination of cocaine in confiscated samples, *Electroanalysis* **3**, 1991, 409-412.
- [7] P. Abad-Valle, M.T. Fernández-Abedul and A. Costa-García, Genosensor on gold films with enzymatic electrochemical detection of a SARS virus sequence, *Biosens. Bioelectron.* **20**, 2005, 2251-2260.
- [8] R. García-González, M.T. Fernández-Abedul, A. Pernía and A. Costa-García, Electrochemical characterization of different screen-printed gold electrodes, *Electrochim. Acta* **53**, 2008, 3242-3249.
- [9] R. García-González, A. Costa-García and M.T. Fernández-Abedul, Dual screen-printed electrodes with elliptic working electrodes arranged in parallel or perpendicular to the strip, *Sensors Sens. Actuators B* **198**, 2014, 302-308.
- [10] A.C. Glavan, D.C. Christodouleas, B. Mosadegh, H.D. Yu, B.S. Smith, J. Lessing, M.T. Fernández-Abedul and G.M. Whitesides, Folding analytical devices for electrochemical ELISA in hydrophobic R(H) paper, *Anal. Chem.* **86**, 2014, 11999-12007.

- [11] A.W. Martinez, S.T. Phillips, M.J. Butte and G.M. Whitesides, Patterned paper as a platform for inexpensive low-volume, portable bioassays, *Angew. Chemie* - *Int. Ed.* **46**, 2007, 1318-1320.
- [12] W. Dungchai, O. Chailapakul and C.S. Henry, Electrochemical detection for paper-based microfluidics, *Anal. Chem.* **81**, 2009, 5821-5826.
- [13] Z. Nie, C.A. Nijhuis, J. Gong, X. Chen, A. Kumachev, A.W. Martinez, M. Narovlyansky and G.M. Whitesides, Electrochemical sensing in paper-based microfluidic devices, *Lab Chip* **10**, 2010, 477-483.
- [14] C. Renault, X. Li, S.E. Fosdick and R.M. Crooks, Hollow-channel paper analytical devices, *Anal. Chem.* **85**, 2013, 7976-7979.
- [15] E. Núñez-Bajo, M. Carmen Blanco-López, A. Costa-García and M. Teresa Fernández-Abedul, Integration of gold-sputtered electrofluidic paper on wire-included analytical platforms for glucose biosensing, *Biosens. Bioelectron.* **91**, 2017, 824-832.
- [16] J.P. Metters, S.M. Houssein, D.K. Kampouris and C.E. Banks, Paper-based electroanalytical sensing platforms, *Anal. Methods* **5**, 2013, 103-110.
- [17] J. Mettakoonpitak, K. Boehle, S. Nantaphol, P. Teengam, J.A. Adkins, M. Srisa-Art and C.S. Henry, Electrochemistry on paper-based analytical devices: a review, *Electroanalysis* **28**, 2016, 1420-1436.
- [18] J.C. Cunningham, P.R. DeGregory and R.M. Crooks, New functionalities for paper-based sensors lead to simplified user operation, lower limits of detection, and new applications, *Annu. Rev. Anal. Chem.* **9**, 2016, 183-202.
- [19] Y. Yang, E. Noviana, M.P. Nguyen, B.J.G. Eiss, D.S. Dandy and C.S. Henry, Paper-based microfluidic devices: emerging themes and applications, *Anal. Chem.* **89**, 2017, 71-91.
- [20] S.E. Fosdick, M.J. Anderson, C. Renault, P.R. DeGregory, J.A. Loussaert and R.M. Crooks, Wire, mesh, and fiber electrodes for paper-based electroanalytical devices, *Anal. Chem.* **86**, 2014, 3659-3666.
- [21] O. Amor-Gutiérrez, E. Costa-Rama, A. Costa-García and M.T. Fernández-Abedul, Paper-based maskless enzymatic sensor for glucose determination combining ink and wire electrodes, *Biosens. Bioelectron.* **93**, 2016, 40-45.
- [22] S. Cinti, D. Talarico, G. Palleschi, D. Moscone and F. Arduini, Novel reagentless paper-based screen-printed electrochemical sensor to detect phosphate, *Anal. Chim. Acta* **919**, 2016, 78-84.
- [23] E. Núñez-Bajo, M.C. Blanco-López, A. Costa-García and M.T. Fernández-Abedul, Electrogeneration of gold nanoparticles on porous-carbon paper-based electrodes and application to inorganic arsenic analysis by chronoamperometric stripping in white wines, *Anal. Chem.* 2017, [accepted \(in press\)](#).
- [24] A.C. Siegel, S.T. Phillips, M.D. Dickey, N. Lu, Z. Suo and G.M. Whitesides, Foldable printed circuit boards on paper substrates, *Adv. Funct. Mater.* **20**, 2010, 28-35.
- [25] R.F. Carvalhal, M.K. Simão, M.H.P. de Oliveira, A.L. Gobbi and L.T. Kubota, Electrochemical detection in a paper-based separation device, *Anal. Chem.* **82**, 2010, 1162-1165.
- [26] P. Ihalainen, A. Määttänen, M. Pesonen, P. Sjöberg, J. Sarfraz, R. Österbacka and J. Peltonen, Paper-supported nanostructured ultrathin gold film electrodes - [Characterization](#) and functionalization, *Appl. Surf. Sci.* **329**, 2015, 321-329.
- [27] M.M. Hamed, B. Ünal, E. Kerr, A.C. Glavan, M.T. Fernández-Abedul and G.M. Whitesides, Coated and uncoated cellophane as materials for microplates and open-channel microfluidics devices, *Lab Chip* **16**, 2016, 3885-3897.
- [28] Y. Wu, P. Xue, Y. Kang and K.M. Hui, Paper-based microfluidic electrochemical immunodevice integrated with nanobioprobes onto graphene film for ultrasensitive multiplexed detection of cancer biomarkers, *Anal. Chem.* **85**, 2013, 8661-8668.
- [29] G. Sun, L. Zhang, Y. Zhang, H. Yang, C. Ma, S. Ge, M. Yan, J. Yu and X. Song, Multiplexed enzyme-free electrochemical immunosensor based on ZnO nanorods modified reduced graphene oxide-paper electrode and silver deposition-induced signal amplification strategy, *Biosens. Bioelectron.* **71**, 2015, 30-36.
- [30] D. Hernández-Santos, M.B. González-García and A. Costa-García, Metal-nanoparticles based electroanalysis, *Electroanalysis* **14**, 2002, 1225-1235.
- [31] S.Y. Oh, J. Kim and Y. Kim, Paper-based synthesis of Pd-dendrite supported porous gold, *Mater. Lett.* **154**, 2015, 60-63.
- [32] S. Ge, W. Liu, L. Ge, M. Yan, J. Yan, J. Huang and J. Yu, In situ assembly of porous Au-paper electrode and functionalization of magnetic silica nanoparticles with HRP via click chemistry for Microcystin-LR immunoassay, *Biosens. Bioelectron.* **49**, 2013, 111-117.

- [33] G. Sun, Y.-N. Ding, C. Ma, Y. Zhang, S. Ge, J. Yu and X. Song, Paper-based electrochemical immunosensor for carcinoembryonic antigen based on three dimensional flower-like gold electrode and gold-silver bimetallic nanoparticles, *Electrochim. Acta* **147**, 2014, 650-656.
- [34] C.D. Bain, E.B. Troughton, Y.-T. Tao, J.J. Evall, G.M. Whitesides and R.G. Nuzzo, Formation of monolayer films by the spontaneous assembly of organic thiols from solution onto gold, *J. Am. Chem. Soc.* **111**, 1989, 321-335
- [35] F. Lucarelli, G. Marrazza, A.P.F. Turner and M. Mascini, Carbon and gold electrodes as electrochemical transducers for DNA hybridisation sensors, *Biosens. Bioelectron.* **19**, 2004, 515-530.
- [36] C.M. Welch, O. Nekrassova and R.G. Compton, Reduction of hexavalent chromium at solid electrodes in acidic media: reaction mechanism and analytical applications, *Talanta* **65**, 2005, 74-80.
- [37] C. Rong and F.C. Anson, Spontaneous adsorption of heteropolytungstates and heteropolymolybdates on the surfaces of solid electrodes and the electrocatalytic activity of the adsorbed anions, *Inorg. Chim. Acta* **242**, 1996, 11-16.
- [38] W. Wang, L. Kong, J. Zhu and L. Tan, One-pot preparation of conductive composite containing boronic acid derivative for non-enzymatic glucose detection, *J. Colloid Interface Sci.* **498**, 2017, 1-8.
- [39] J.G. Ayenimo and S.B. Adeloju, Amperometric detection of glucose in fruit juices with polypyrrole-based biosensor with an integrated permselective layer for exclusion of interferences, *Food Chem.* **229**, 2017, 127-135.
- [40] B. Pérez-Fernández, D. Martín-Yerga and A. Costa-García, Electrodeposition of nickel nanoflowers on screen-printed electrodes and its application to non-enzymatic determination of sugars, *RSC Adv.* **6**, 2016, 83748-83757.
- [41] Y. Li, Y.-Y. Song, C. Yang and X.-H. Xia, Hydrogen bubble dynamic template synthesis of porous gold for nonenzymatic electrochemical detection of glucose, *Electrochem. Commun.* **9**, 2007, 981-988.
- [42] M. Pasta, F. La Mantia and Y. Cui, Mechanism of glucose electrochemical oxidation on gold surface, *Electrochim. Acta* **55**, 2010, 5561-5568.
- [43] A.-N. Kawde, M.A. Aziz, M. El-Zohri, N. Baig and N. Odewunmi, Cathodized gold nanoparticle-modified graphite pencil electrode for non-enzymatic sensitive voltammetric detection of glucose, *Electroanalysis* **29**, 2017, [available online](#)([available online](#)).
- [44] J.-J. Yu, S. Lu, J.-W. Li, F.-Q. Zhao and B.-Z. Zeng, Characterization of gold nanoparticles electrochemically deposited on amine-functioned mesoporous silica films and electrocatalytic oxidation of glucose, *J. Solid State Electrochem.* **11**, 2007, 1211-1219.
- [45] G. Martínez-Paredes, M.B. González-García and A. Costa-García, Lead sensor using gold nanostructured screen-printed carbon electrodes as transducers, *Electroanalysis* **21**, 2009, 925-930.
- [46] ~~Electroanalytical~~ F. Scholtz, (Ed), ~~Methods~~ *Electroanalytical Methods: Guide to Experiments and applications*, 2002, Springer; Berlin.

Graphical abstract



[alt-text: fx1](#)

Highlights

- Paper-based electrochemical cell with nanostructured gold ~~films~~films.
 - Gold nanoparticles electrogenerated on gold-sputtered paper-based ~~electrodes~~electrodes.
 - Simple and low cost paper-based metallic electrode for sensitive ~~electroanalysis~~electroanalysis.
 - Non-enzymatic determination of glucose with paper-based nanostructured gold ~~platforms~~platforms.
-

Queries and Answers

Query:

Please confirm that given names and surnames have been identified correctly and are presented in the desired order, and please carefully verify the spelling of all authors.

Answer: The given names and surnames are correct and presented in the desired order

Query:

Your article is registered as a regular item and is being processed for inclusion in a regular issue of the journal. If this is NOT correct and your article belongs to a Special Issue/Collection please contact r.saravanakumar@elsevier.com immediately prior to returning your corrections.

Answer: The article is a regular item

Query:

Please verify if the designated corresponding author and email address are correct.

Answer: The designated corresponding author and email address are correct

Query:

Please complete and update the reference given here [23]. For references to articles that are to be included in the same (special) issue, please add the words 'this issue' wherever this occurs in the list and, if appropriate, in the text.

Answer: The article was published in print (20 June 2017) Anal. Chem. 89, 2017, 6415-6423